**2024 NDIA MICHIGAN CHAPTER
GROUND VEHICLE SYSTEMS ENGINEERING
AND TECHNOLOGY SYMPOSIUM
MODELING, SIMULATION, PROTOTYPING & VALIDATION (MSPV)
TECHNICAL SESSION
AUGUST 13-15, 2024 - NOVI, MICHIGAN**

Characterizing and Modeling Lightweight Structural Composites at High Strain Rates for use from Arctic to Desert Environments

Robert J. Hart, PhD[1], Evan G. Patton, PhD[1], Joseph M. Hamilton[2], Isabela Cardenas[2], Huiyang Luo, PhD[2], Joseph Magallanes[2]

[1]US Army DEVCOM Ground Vehicle Systems Center, Warren, MI
[2]Karagozian & Case, Glendale, CA

ABSTRACT

In this work, triaxial carbon fiber – epoxy composite laminates were manufactured and tested to determine the influence of environmental temperature and strain rate on the mechanical properties, and finite element models were developed to understand how those temperature and strain rate dependent trends may influence performance in a military ground vehicle application. As environmental temperature increased, the strength and elastic modulus were observed to decrease. Across all three environmental temperatures tested in this study, as the strain rate increased, tensile strength and elastic modulus were observed to increase as well. When applied to a composite hat section geometry, the finite element results highlighted the importance of considering both the environmental temperature and loading rate in the design of composite structures for use in military ground vehicles.

Citation: R. Hart, E. Patton, J. Hamilton, I. Cardenas, H. Luo, J. Magallanes, "Characterizing and Modeling Lightweight Structural Composites at High Strain Rates for use from Arctic to Desert Environments," In *Proceedings of the Ground Vehicle Systems Engineering and Technology Symposium* (GVSETS), NDIA, Novi, MI, Aug. 13-15, 2024.

1. INTRODUCTION

In the commercial automotive industry, vehicle lightweighting is critical in order to meet ever increasing emissions standards. Each pound of weight saved in a commercial vehicle can be attributed to an incremental increase in fuel efficiency and therefore, there is a defined cost tolerance for each pound of weight savings [1] [2]. In military ground vehicles, weight savings still influences fuel efficiency, however lightweighting tradeoffs are typically made due to "hard point" performance requirements, and not for incremental increases in fuel efficiency [3] [4]. Fiber-reinforced composites have low density and high material stiffness and strength, and therefore have potential to provide significant weight savings, which can then be used to make a vehicle lighter weight or traded for adding more capability to the vehicle. Lightweight composite materials are primarily sought out for military ground vehicles in two applications: (i) B-kit armor packages and (ii) secondary non-ballistic structures. Composite armor solutions are typically selected over metallic solutions because the areal density of the composite armor is less than the metallic solution for a given performance requirement. For secondary structural applications, such as non-ballistic structures inside of a combat vehicle, weight savings is achieved through a combination of design optimization, low material density, and high material stiffness and strength.

Composite laminates can have strength and stiffness similar to metal alloys, but have lower density and thus can often be used to make lighter structural components. Recent efforts have shown that structural thermoplastic composites could be used to make a lightweight tactical cargo shell that saves 35% of weight compared to aluminum [5]. In a combat vehicle crew floor application, weight savings was 56% compared to a baseline aluminum design [6]. Weight savings was achieved in these secondary structural applications (i.e. not part of the primary vehicle structure) through a combination of design optimization, low material density of the composite, and high structural performance (*i.e.*, high specific stiffness and strength). In addition to lightweighting benefits, when designed properly, composite materials can provide superior energy absorption due to their complex failure mechanisms. For example, under axial crushing during a vehicle crash event, composite structures are able to absorb more energy using less mass when compared to sheet metal structures.

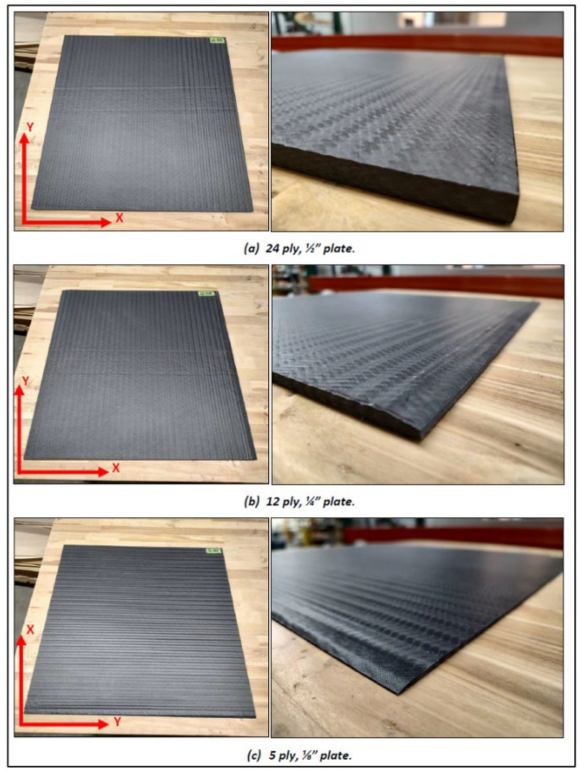

Figure 1: Images of triaxial carbon fiber / epoxy panels manufactured using vacuum assisted resin transfer molding process.

This trend has been shown to hold true for both thermoset [7, 8] and thermoplastic [9, 10, 11] composites.

One challenge with military ground vehicles is that unlike passenger vehicles, military vehicles are not developed to operate on road in a particular climate but are instead expected to perform fully operational from extreme arctic to arid desert environments while simultaneously being subject to severe dynamic events, such a gunfire loading, ballistic impacts, and blast. Fiber-reinforced polymer (FRP) composite laminates, such as fiberglass-epoxy and carbon fiber-epoxy composites have been known to exhibit temperature dependent and strain rate dependent material properties, so in order to utilize these lightweight composites in more military ground vehicle applications, the defense

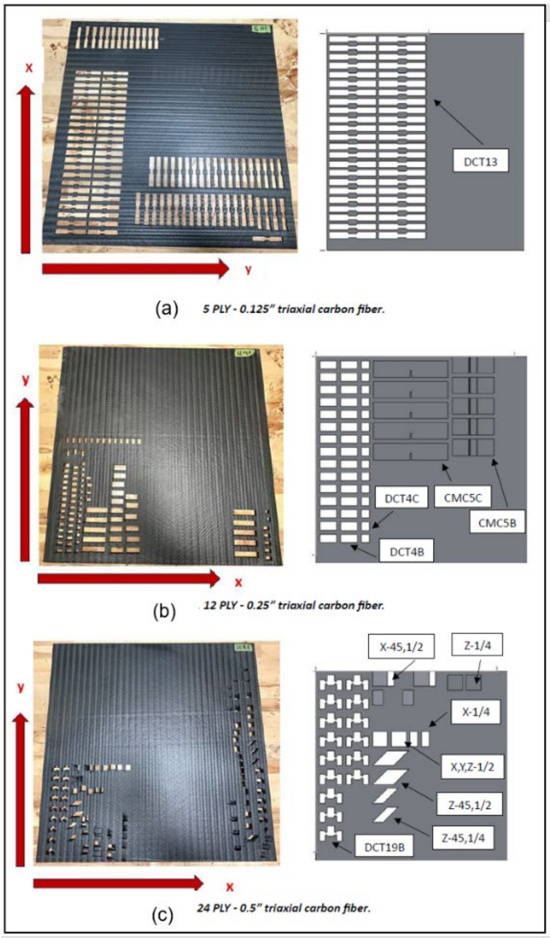

Figure 2: Schematic of mechanical characterization test specimens cut from (a) 1/8" thick, (b) ¼" thick, and (c) ½" thick panels.

industry must understand how these materials will perform across all operational environments.

This study has focused on gaining greater understanding into the temperature-dependent and strain-rate dependent mechanical properties of a triaxial carbon fiber – epoxy composite that has potential for reducing the weight of secondary structures in military ground vehicles. Mechanical characterization tests were performed from -60 °F (representing extreme artic conditions) to 180 °F (representing arid desert conditions) and at strain rates from 0.01 s^{-1} (quasi-static) to 1,000 s^{-1} (dynamic).

2. METHODS

2.1. Composite Manufacturing

The composite laminate tested in this study utilized a triaxial braided fabric, QISO-HW-48, from A&P Technology. The fabric consists of T-700 SC 12K 50C fibers braided into a single layer, balanced 0, +/-60 fiber architecture. The fabric was laminated into panels using SC-15 toughened epoxy resin and processed using vacuum assisted resin transfer molding and post oven cure cycle. Panels were manufactured to nominal thicknesses of 1/8", ¼", and ½" (see Figure 1) in order to satisfy the geometry requirements of the mechanical characterization testing.

2.2. Mechanical Characterization

The primary purpose of this research effort was to understand the influence of strain rate (0.01 s^{-1} to 1,000 s^{-1}) and environmental temperature (-60 °F to 180 °F) on the structural performance of the triaxial carbon fiber / epoxy composite laminate. In order to utilize material characterization data in a modeling and simulation environment, the elastic properties and failure limits must be understood in tension, compression, and shear for the range of strain rates and environmental conditions expected in vehicle operation. Therefore, a series of tensile, compression, shear, and mode I & II fracture tests were performed at strain rates of 0.01 s^{-1}(Quasi-Static, QS), 1 s^{-1} (Quasi-Dynamic, QD), and 1,000 s^{-1} (Dynamic, D), with each test repeated under environmental temperatures of -60 °F (referred to as low temperature, or LT), Room Temperature (RT), and 180 °F (referred to as high temperature, HT). A servo electric test module was utilized for lower strain rate

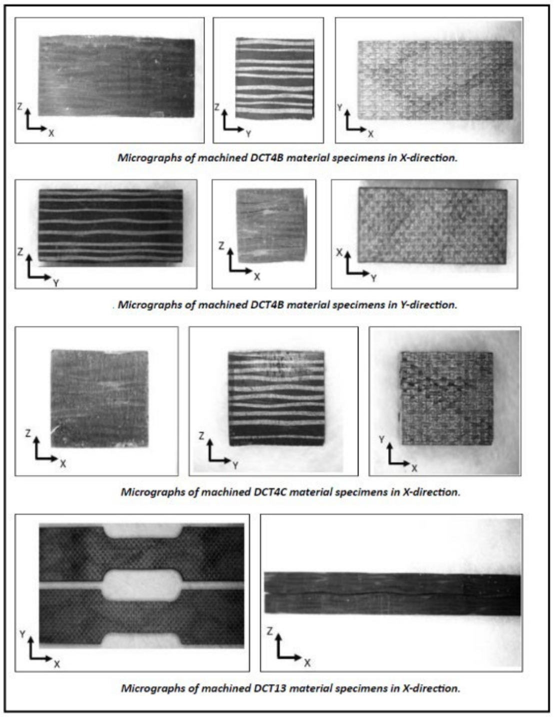

Figure 3: Computed tomography micrographs showing internal fiber architecture of specimens.

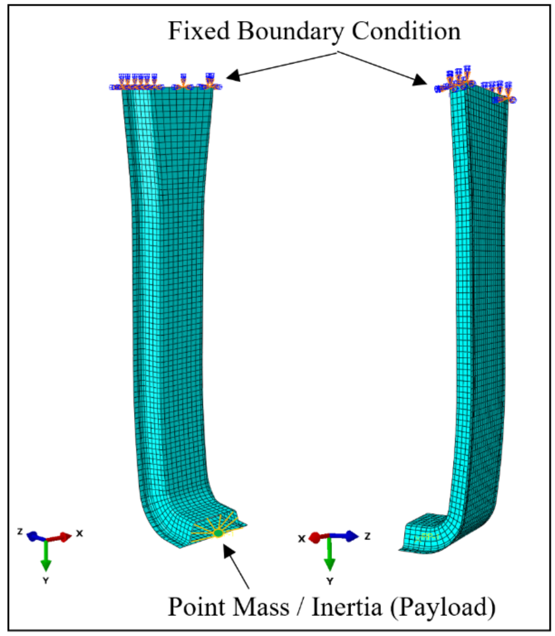

Figure 4: Mesh of Generalized Composite Hat Section Showing Location of Point Mass / Inertia (Payload) and Fixed Boundary Condition.

testing, while a split-Hopkinson pressure/tension bar (SHPB/SHTB) was utilized to gather high strain rate data. In each test setup, environmental chambers were utilized to isolate and control the environmental temperature during each test.

In addition, ultrasonic non-destructive test (NDT) methods were also utilized to measure material elastic properties, using the transmission method, longitudinal wave (P-wave) speeds and shear wave (S-wave) speeds were measured on two different thickness cuboid samples. The ultrasonic NDT methods were intended to verify the assumption that the triaxial carbon fiber weave produces a nearly isotropic material, which is advertised by vendors. Results of the NDT tests indicated that there may be some anisotropy between x and y - directions, but due to the limited number of test specimens in this study, the assumption of isotropic material properties was carried forward into the finite element methods.

2.3. Finite Element Methods

In order to understand the effects of temperature and rate-dependent material properties on a vehicle application, a generalized composite vehicle structure was analyzed. For this study, a hat section type of structure was selected, which includes relevant design features and geometry that could apply to a structural member within a military ground vehicle. The generalized composite structure in Figure 4 enables researchers to evaluate the relationship between a composite material, manufacturing process, and performance on a 3-dimensional structure, which may be more representative of a molded component, compared to a traditional flat laminated plate.

The generalized structure was modeled in Abaqus CAE with 3-D solid shell elements, and the elastic properties were assigned as determined from the tension and

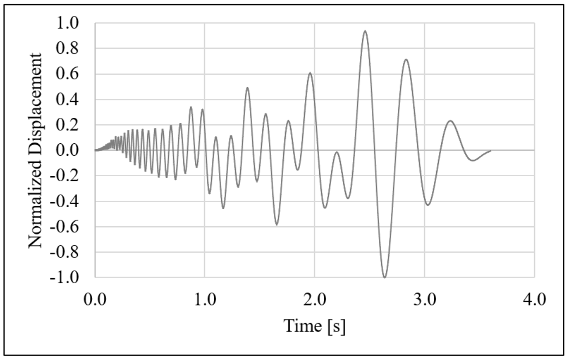

Figure 5: Generalized Shock Profile Applied to the Y-Direction Boundary Condition within Linear Perturbation Step of FE model.

compression tests. One end of the structure utilized fixed boundary conditions, representing a bonded joint to the vehicle structure, whereas the other end of the structure was connected to a point mass/inertia, representing the payload connected to the composite structure. Both "static" and "shock" loads were applied to the structure in separate analyses in order to understand the structure's response under general mobility loads and more severe shock loads. The static analyses were conducted by applying a G-load multiplication factor to the payload in the vertical direction (y-direction in Figure 4), where as the shock analyses were conducted through a linear-perturbation procedure with the shock load being applied as a displacement-based perturbation on the fixed boundary condition in the vertical direction (y-direction in Figure 4). Figure 5 shows a profile of the generalized shock perturbation applied in the finite element model. It is important to note that in order to run a shock analyses in Abaqus, the analysis must be run as a modal dynamics step type under the linear perturbation procedure, and prior to the modal dynamics step (shock step), a frequency step must be conducted in order to solve for the mode shapes and frequencies. In this study, a frequency step (modal analysis) was conducted to obtain frequencies and mode shapes of the first 6 eigenvalues, which was followed by the modal dynamics step in order to observe the response of the structure to the shock perturbation in Figure 5. The static analyses were performed using quasi-static (QS) test data at 0.01 s^{-1} and repeated using material properties at LT, RT, and HT. The modal dynamics analyses (shock analyses) were conducted using the quasi-dynamic (QD) test data at 1 s^{-1}. The strain rate field variable is not available in a modal dynamics analyses, but strain rates were approximated using change in strain over change in time, and the QD strain rate was determined to be most appropriate for the shock analyses.

3. RESULTS AND DISCUSSION

3.1. Mechanical Characterization

3.1.1 Influence of Strain Rate

In order to understand the influence of strain rate on mechanical response, the results of tensile tests were plotted in Figure 6 simultaneously for tests conducted at strain rates of 0.01 s^{-1}, 1 s^{-1}, and 1,000 s^{-1}. As seen in Figure 6 (a), at room temperature, the slope of the initial elastic region was highest in the 1,000 s^{-1} test (highest elastic modulus) and the tensile strength was also highest in the high strain rate test. This trend continued for the HT and LT tests, where in both of these tests, the highest elastic modulus and tensile strength were observed in the 1,000 s^{-1} tensile test. Across all environmental temperatures tested in this study, as the strain rate increased, tensile strength was observed to increase as well. The effect of strain rate on elastic modulus was not so clearly evident when comparing the 0.01 s^{-1} and 1 s^{-1} tests, however when increasing from 1 s^{-1} to 1,000 s^{-1}, the elastic modulus clearly increased with strain rate. This trend may indicate that for FE models where low strain rates are expected and the response is kept well within the elastic regime, elastic

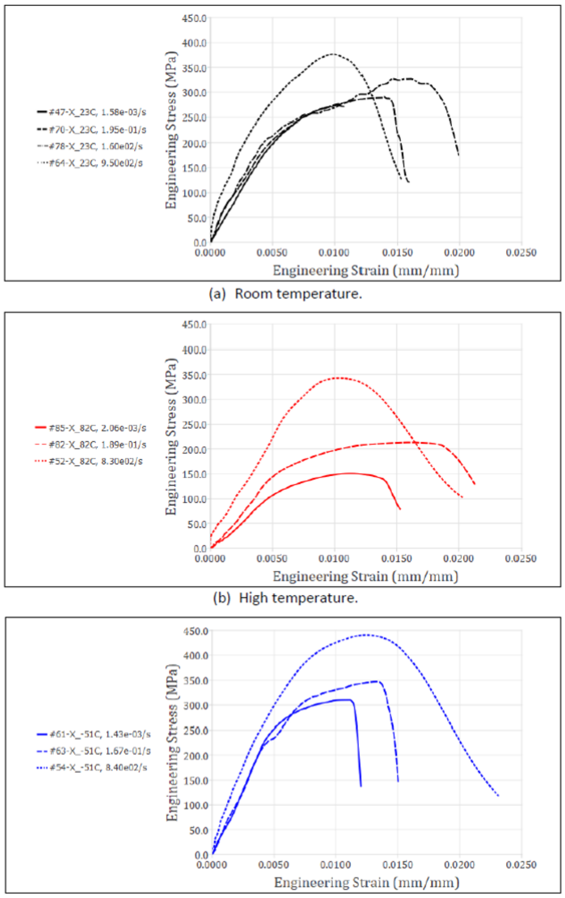

(a) Room temperature.

(b) High temperature.

(c) Low temperature.

Figure 6: Comparison of stress-strain curves under varying strain rates for tensile tests conducted in the x-direction at (a) room temperature, (b) high temperature, and (c) low temperature.

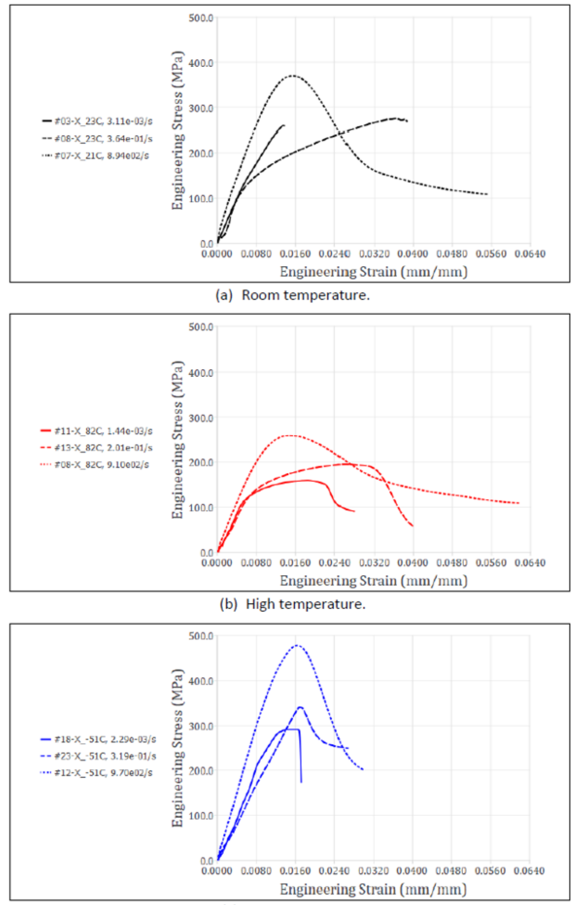

(a) Room temperature.

(b) High temperature.

(c) Low temperature.

Figure 7: Comparison of stress-strain curves under varying strain rates for compression tests conducted in the x-direction at (a) room temperature, (b) high temperature, and (c) low temperature.

modulus from a quasi-static test may be sufficient, however for higher strain rate events and highly dynamic analyses, high strain rate properties may be required in order to model an accurate response. Similar results were observed in compression test results in Figure 7.

For compression tests, the highest compression strength was observed under the 1000 1 s^{-1} test, and lowest compression strength was observed at the lowest strain rate of 0.01 1 s^{-1}. It is important to note that there was good agreement in the elastic modulus observed in both the tensile and compression tests in Figures 6 and 7, which is important to check because certain composite laminates and fabrics have been observed to have different elastic responses in tension and compression, due to factors such as fiber misalignment or manufacturing defects [12]. In this case, having similar elastic response in tension and compression is an indicator of a high quality composite laminate and greatly simplifies FE modeling.

3.1.2 Influence of Temperature

When observing the effects of temperature on elastic modulus, compression strength, and tensile strength in Figures 8 and 9, some noteworthy trends can be elucidated. At a given strain rate, the lowest elastic modulus and lowest strength was observed in the high temperature test,

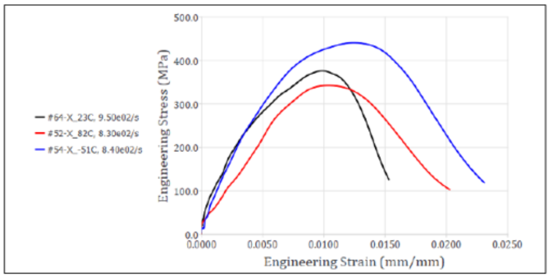

(a) x-direction tension tests at 1,000 /s

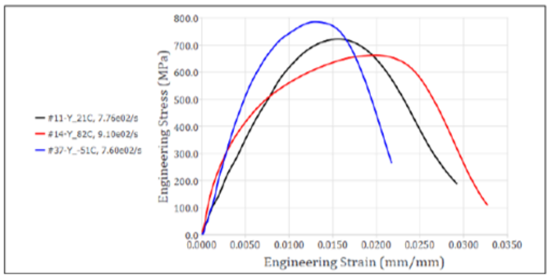

(b) y-direction tension tests at 1,000 /s

Figure 8: Comparison of stress-strain curves under varying environmental temperatures for tensile tests (a) conducted in the x-direction at 1000 / s strain rate and (b) conducted in the y-direction at 1000 / s strain rate.

and the highest modulus and strength was observed in the low temperature test. When applying this to a structural application in a ground vehicle, it suggests that in order to accurately design around the most conservative safety factor, for this material (and other similar composites experiencing the same temperature-dependent effects), the material properties at the highest operational temperature should be used in the FE model. In order to verify this hypothesis, FE models were run using data from all three environmental temperature conditions in order to see practical implications of one temperature-based model compared to another.

3.1.3 Mechanical Properties

The mechanical properties of the composite material were extracted from the curves in Figures 6-9, and are shown in

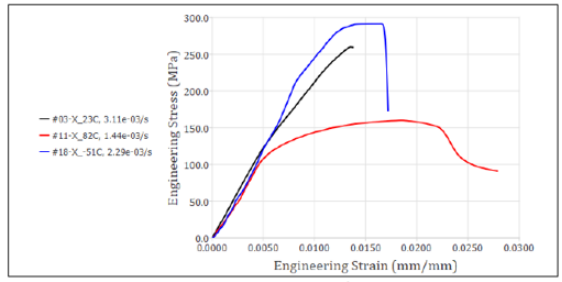

(a) Strain-rate: 0.01/s.

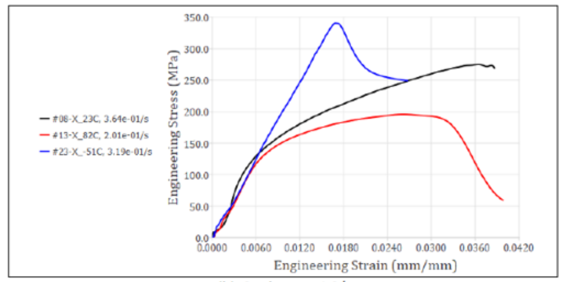

(b) Strain-rate: 1.0/s.

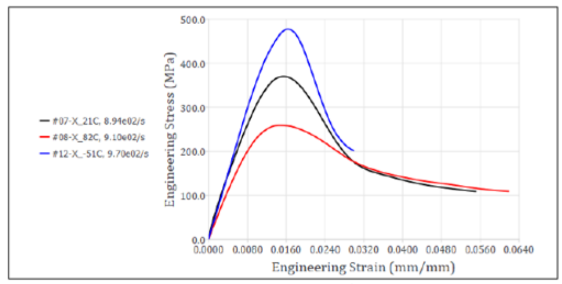

(c) Strain-rate: 1,000/s.

Figure 9: Comparison of stress-strain curves under varying environmental temperatures for compression tests conducted in the x-direction at (a) 0.01 / s strain rate, (b) 1.0 / s strain rate, and (c) 1000 / s strain rate.

Table 1. It is important to note that these mechanical properties are determined from single coupon tests, and have not been characterized extensively enough to determine statistical significance. Under this context, these properties were used within this study to observed how the temperature and strain rate trends discussed above impact performance in a structural application in a military environment.

Table 1. Mechanical Property Data for various Strain-Rates and Environmental Temperatures, Based on Single Test Curves in Figures 6-9

Density [g/cc]	1.513		
	Quasi-Static (QS)		
	LT_QS	RT_QS	HT_QS
Elastic Modulus [GPa]	53.4	42.7	21.5
Tensile Strength [MPa]	313.2	277.0	152.6
Compressive Strength [MPa]	286.9	256.4	157.0
	Quasi-Dynamic (QD)		
	LT_QD	RT_QD	HT_QD
Elastic Modulus [GPa]	53.2	49.4	27.8
Tensile Strength [MPa]	351.1	294.5	216.7
Compressive Strength [MPa]	328.7	265.1	190.7
	Dynamic (D)		
	LT_D	RT_D	HT_D
Elastic Modulus [GPa]	62.9	61.2	41.6
Tensile Strength [MPa]	446.3	380.3	346.1
Compressive Strength [MPa]	470.0	271.0	255.4

3.2. Finite Element Results

3.2.1 Static Analysis

The static analyses were conducted by applying a G-load multiplication factor to the payload in the vertical direction (y-direction in Figure 4) and the results are shown in Table 2 and Figure 10. One of the first observations that can be noticed is that as temperature increases from low temperature (LT) to room temperature (RT) to high temperature (HT), the maximum deflection of the composite structure increased. This result follows intuition, since previously it was observed that elastic modulus decreased with increasing temperature. It was also observed in the FE analyses that as temperature increased, maximum principal stress decreased, however the rate at which the maximum principal stress decreased was less than the drop in tensile strength due to temperature. This trend resulted in the lowest safety factor in tension of 2.0 for the static, high temperature analysis, based on the Maximum Principal Stress criteria, which is a comment failure criteria for fiber reinforced composite materials. It should be noted that in all static analyses, the maximum principal stress was observed on the outer surface of the curved portion of the hat section, as shown in Figure 10 (a) – (c), where as the minimum principal stress was observed at the same location, but on the inner surface of the composite laminate. For all three static analyses conducted, the safety factor in compression was higher than the safety factor in tension.

Table 2. FE Results for Static Load Case (Positive Mobility G Load)

	LT_QS	**RT_QS**	**HT_QS**
Maximum Deflection [mm]	7.42	8.98	15.6
Maximum Principal Stress [MPa]	81.6	81.3	77.0
Tensile Strength [MPa]	313.2	277.0	152.6
Safety Factor (Tension)	3.8	3.4	2.0
Minimum Principal Stress (Abs Value) [MPa]	33.2	33.0	32.5
Compressive Strength [MPa]	286.9	256.4	157.0
Safety Factor (Compression)	8.6	7.8	4.8

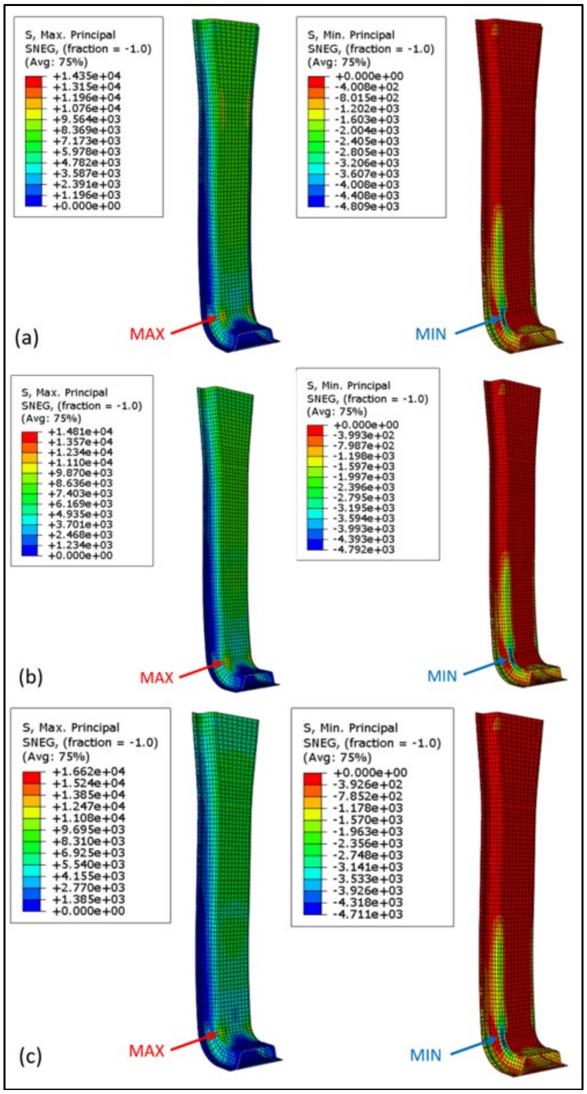

Figure 10: Maximum and minimum principal stresses in the composite hat section for static analysis (units of stress are in PSI)

3.2.2 Shock Analysis Using Modal Dynamics Load Step

In order to conduct a shock analysis in Abaqus, the modal dynamics load step must be preceded by a frequency analysis (modal analysis), which determines the mode shapes and associated frequencies of the composite hat section. The first six mode shapes and frequencies are shown in Figure 11. After the frequency analysis, the modal dynamics load step was conducted, and the displacement versus time shock profile in Figure 5 was applied as a displacement-based perturbation in the y-direction on the fixed boundary condition. The modal dynamics analysis required approximately 30 minutes to run on a PC using 4 processors, and consisted of approximately 17,500 time steps. In order to evaluate maximum deflection, maximum principal stress, and minimum principal stresses throughout the entire analysis, a frame-based field output was created so that at each node, the maximum (or minimum) value of the deflection and stress results were recorded from the maximum value observed over the 17,500 frames, and the results are shown in Figure 12 and Table 3.

Similar to the static analysis, the maximum and minimum principal stresses were observed at the same location within the curved section of the part, as seen in Figure 12. Also, similar to the static analyses, as temperature increased, maximum deflection increased. However, when observing principal stresses, the highest principal stresses were observed in the high temperature test. This result is particularly noteworthy, because the high temperature condition resulted in the lowest quasi-dynamic material strength, meaning that with the higher stresses and lower material strength in the high temperature condition, the safety factor was adversely affected.

When observing safety factor, across all shock analyses at low, room, and high temperature, the safety factors were all lower than the corresponding static analyses. The high temperature condition resulted in the lowest safety factors in both static and shock analyses, with the safety factor reaching values of 0.9 and 0.7 in tension and compression, respectively. This result indicates that the failure criteria have been reached locally within the composite hat section at the high temperature condition,

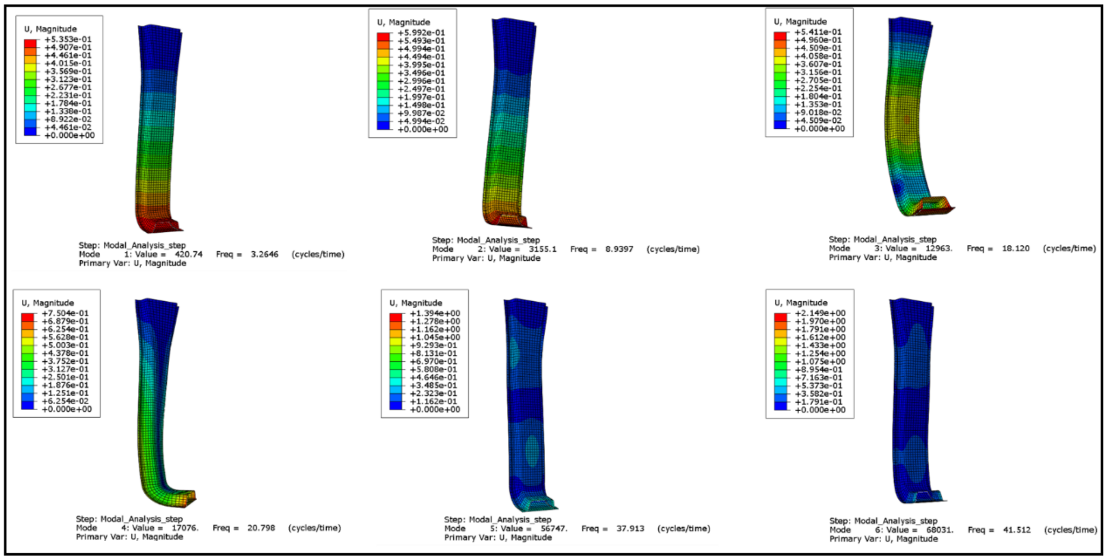

Figure 11: First six mode shapes and frequencies from modal analysis step (units of deflection are in inches)

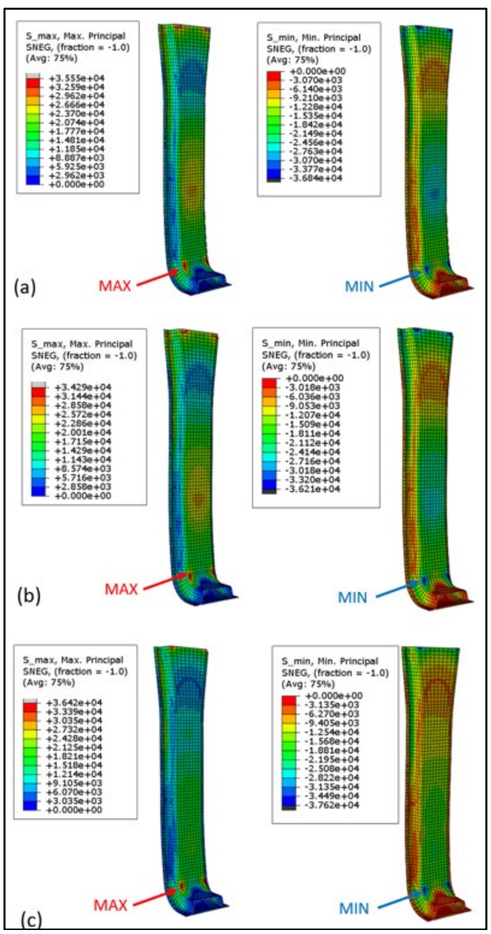

Figure 12: Maximum and minimum principal stresses at (a) Low, (b) Room, and (c) High Temperature (units of stress are in PSI)

Table 3. FE Results for Shock Load Case using Shock Profile in Figure 5

	LT_QD	RT_QD	HT_QD
Maximum Deflection [mm]	7.42	7.63	11.4
Maximum Principal Stress [MPa]	245.1	236.4	251.1
Tensile Strength [MPa]	351.1	294.5	216.7
Safety Factor (Tension)	1.4	1.2	0.9
Minimum Principal Stress (Abs Value) [MPa]	254	249.7	259.4
Compressive Strength [MPa]	328.7	265.1	190.7
Safety Factor (Compression)	1.3	1.1	0.7

where as in room temperature and low temperature conditions, the safety factors were all greater than 1.0. This result illuminates the importance of considering operating environmental temperature in addition to loading conditions when optimizing the design of structural composites for use in military ground vehicles. If the design only accounts for static analyses or ignores elevated temperature conditions, the design would not be accurately optimized to true operating conditions. It should be noted that these analyses and results should be kept within the context of this limited strain-rate and temperature dependent research study and should not be generalized for all fiber-reinforced composites used in military ground vehicle applications. For instance, not all resin systems will response in the same manner to strain-rate and temperature effects, and the high temperature condition of 180° may be higher than actual operating conditions for applications in some areas of the vehicle.

4. CONCLUSIONS

In this work, triaxial carbon fiber – epoxy composite laminates were manufactured and tested to determine the influence of environmental temperature and strain rate on the mechanical properties. As environmental temperature increased, the strength and elastic modulus were observed to decrease. When applying this to a structural application in a ground vehicle, it suggests that in order to accurately design around the most conservative safety factor, for this material (and other similar composites experiencing the same temperature-dependent effects), the material properties at the highest operational temperature should be used in the FE model.

Across all three environmental temperatures tested in this study, as the strain rate increased, tensile strength was observed to increase as well. The effect of strain rate on elastic modulus was not so clearly evident when comparing the 0.01 s^{-1} 1 s^{-1} tests, however when increasing from 1 s^{-1} to 1,000 s^{-1}, the elastic modulus clearly increased with strain rate. When applied to the static and shock analyses of the composite hat section structure, the strain rate-dependent and temperature-dependent properties resulted in some noteworthy trends. Most noteworthy, in the shock analyses, the maximum principal stresses were higher compared to the static analyses at the same temperature, however the highest stresses were observed in the high temperature shock analysis, resulting in the lowest safety factors in tension and compression.

These trends may indicate that for FE models where low strain rates are expected and the response is kept well within the elastic regime, elastic modulus from a quasi-static test may be sufficient, however for higher strain rate events and highly dynamic analyses, high strain rate dependent properties may be required in order to model an accurate response. Regardless of the strain-rate effect, the results highlighted the importance of characterizing material properties under the range of environmental temperatures expected, and in this study, the highest operational temperature resulted in the lowest observed safety factor.

5. REFERENCES

[1] E. Polsen, L. Krogsrud, R. Carter, W. Oberle, C. Haines and A. Littlefield, "Lightweight Combat Vehicle Science and Technology Campaign," US Army TARDEC, Warren, 2014.

[2] J. Sullivan, G. Keoleian and R. Hart, "Energy, Fuels, and Cost Analyses for the M1A2 Tank: A Weight Reduction Case Study," in *SAE Technical Paper 2020-01-0173*, Detroit, 2020.

[3] R. Gerth and R. Howell, "What Is a Ton of Weight Worth? A Discussion of Military Ground System Weight Considerations," in *SAE Technical Paper 2017-01-0270*, Detroit, 2017.

[4] R. Hart and R. Gerth, "THE INFLUENCE OF GROUND COMBAT VEHICLE WEIGHT ON AUTOMOTIVE PERFORMANCE, TERRAIN TRAVERSABILITY, COMBAT EFFECTIVENESS, AND OPERATIONAL ENERGY," in *Ground Vehicle Systems Engineering Technology Symposium*, Novi, 2018.

[5] D. Erb, B. Dwyer, J. Roy, W. Yori, R. Lopez-Anido, A. Q. Smail and R. J. Hart, "UTILIZING ADDITIVE MANUFACTURING TO ENABLE

LOW-COST, RAPID FORMING OF HIGH TEMPERATURE LIGHTWEIGHT GROUND VEHICLE STRUCTURES," in *Ground Vehicle Systems Engineering and Technology Symposium (GVSETS)*, Novi, 2021.

[6] R. J. Hart, B. Dwyer, A. Q. Smail, A. Chishti, D. Erb and R. Lopez-Anido, "LIGHTWEIGHT COMPOSITE CREW FLOOR FOR GROUND COMBAT," in *Proceedings of the Ground Vehicle Systems Engineering and Technology Symposium (GVSETS)*, Novi, 2021.

[7] D. Shi and X. Xiao, "An enhanced continuum damage mechanics model for crash simulation of composites," *Compos. Struct.,* vol. 185, pp. 774-785, 2017.

[8] A. Cherniaev, C. Butcher and J. Montesano, "Predicting the axial crush response of CFRP tubes using three damage-based constitutive models," *Thin-Walled Struct.,* vol. 129, pp. 349-364, 2018.

[9] NCMS, "High-Performance Computing Studies," 2017.

[10] T. Matsuo, M. F. K. Kan, T. Sumiyama and H. Enomoto, "Predicting the axial crush response of CFRP tubes using three damage-based constitutive models," *Thin-Walled Struct.,* vol. 129, pp. 349-364, 2018.

[11] R. Hart, B. Khatib-Shahidi, E. Patton and A. Smail, "Modeling Dynamic Failure of Woven Carbon Fiber Thermoplastic Composites Using Empirical-and Multiscale-Based Material Cards in LS-DYNA MAT054," *SAE International Journal of Materials and Manufacturing,* vol. 13, no. 05-13-03-0020, pp. 241-255, 2020.

[12] M. Meng, H. Le, M. Rizvi and S. Grove, "The effects of unequal compressive/tensile moduli of composites," *Composite Structures,* vol. 126, pp. 207-215, 2015.